# Multi-resonant metamaterials based on UT-shaped nano-aperture antennas

**Mustafa Turkmen,[1,2,3] Serap Aksu,[3,4] A. E. Çetin,[2,3] A. Ali Yanik,[2,3] and Hatice Altug[2,3,4,*]**

[1]*Electrical and Electronics Engineering, Erciyes University, 38039, Kayseri, Turkey*
[2]*Electrical and Computer Engineering, Boston University, Boston, MA, 02215, USA*
[3]*Photonics Center, Boston University, Boston, MA, 02215, USA*
[4]*Materials Science and Engineering, Boston University, Boston, MA, 02215, USA*
**altug@bu.edu*

**Abstract**: We demonstrate a compact multi-resonant metamaterial structure based on integrated U- and T-shaped nano-aperture antennas. We investigate the physical origin of the multi-resonant behavior and determine the parameter dependence of the nano-aperture antennas both experimentally and numerically. We also show enhanced field distribution in the apertures at the corresponding resonance wavelengths. Both multi-spectral response and enhanced near field distributions can open up exciting new opportunities in applications ranging from subwavelength optics and optoelectronics to chemical and biosensing.



**OCIS codes:** (220.4241) Nanostructure fabrication; (050.6624) Subwavelength structures; (240.6680) Surface plasmons; (060.4510) Optical communications; (130.7408) Wavelength filtering devices; (230.5750) Resonator; (999.9999) Metamaterials.

## References and links

1. J. B. Pendry, D. Schurig, and D. R. Smith, "Controlling electromagnetic fields," Science **312**(5781), 1780–1782 (2006).
2. V. M. Shalaev, "Optical negative-index metamaterials," Nat. Photonics **1**(1), 41–48 (2007).
3. C. M. Soukoulis, S. Linden, and M. Wegener, "Physics. Negative refractive index at optical wavelengths," Science **315**(5808), 47–49 (2007).
4. J. B. Pendry, A. J. Holden, D. J. Robbins, and W. J. Stewart, "Magnetism from conductors and enhanced non-linear phenomena," IEEE Trans. Microw. Theory Tech. **47**(11), 2075–2084 (1999).
5. J. B. Pendry, "Photonics: metamaterials in the sunshine," Nat. Mater. **5**(8), 599–600 (2006).
6. G. Lévêque, and O. J. F. Martin, "Narrow-band multiresonant plasmon nanostructure for the coherent control of light: an optical analog of the xylophone," Phys. Rev. Lett. **100**(11), 117402 (2008).
7. C. Zhu, J.-J. Ma, L. Li, and C.-H. Liang, "Multiresonant Metamaterial Based on Asymmetric Triangular Electromagnetic Resonators," IEEE Antennas Wirel. Propag. Lett. **9**, 99–102 (2010).
8. H. Chen, L. Ran, J. Huangfu, X. Zhang, K. Chen, T. M. Grzegorczyk, and J. A. Kong, "Metamaterial exhibiting left-handed properties over multiple frequency bands," J. Appl. Phys. **96**(9), 5338–5340 (2004).
9. Y. Yuan, C. Bingham, T. Tyler, S. Palit, T. H. Hand, W. J. Padilla, N. M. Jokerst, and S. A. Cummer, "A dual-resonant terahertz metamaterial based on single-particle electric-field-coupled resonators," Appl. Phys. Lett. **93**(19), 191110 (2008).
10. D. Wang, L. Ran, B. I. Wu, H. Chen, J. Huangfu, T. M. Grzegorczyk, and J. A. Kong, "Multi-frequency resonator based on dual-band S-shaped left-handed material," Opt. Express **14**(25), 12288–12294 (2006).
11. D.-H. Kwon, D. H. Werner, A. V. Kildishev, and V. M. Shalaev, "Near-infrared metamaterials with dual-band negative-index characteristics," Opt. Express **15**(4), 1647–1652 (2007).
12. U. K. Chettiar, A. V. Kildishev, H.-K. Yuan, W. Cai, S. Xiao, V. P. Drachev, and V. M. Shalaev, "Dual-band negative index metamaterial: double negative at 813 nm and single negative at 772 nm," Opt. Lett. **32**(12), 1671–1673 (2007).
13. A. Degiron, H. J. Lezec, N. Yamamoto, and T. W. Ebbesen, "Optical transmission properties of a single subwavelength aperture in a real metal," Opt. Commun. **239**(1-3), 61–66 (2004).
14. A. Degiron, and T. W. Ebbesen, "The role of localized surface Plasmon modes in the enhanced transmission of periodic subwavelength apertures," J. Opt. A, Pure Appl. Opt. **7**(2), S90–S96 (2005).
15. M.-W. Tsai, T.-H. Chuang, H.-Y. Chang, and S.-C. Lee, "Bragg scattering of surface plasmon polaritons on extraordinary transmission through silver periodic perforated hole arrays," Appl. Phys. Lett. **88**(21), 213112 (2006).
16. T. Matsui, A. Agrawal, A. Nahata, and Z. V. Vardeny, "Transmission resonances through aperiodic arrays of subwavelength apertures," Nature **446**(7135), 517–521 (2007).
17. J.-B. Masson, and G. Gallot, "Coupling between surface plasmons in subwavelength hole arrays," Phys. Rev. B **73**(12), 121401 (2006).

#142785 - $15.00 USD Received 16 Feb 2011; revised 29 Mar 2011; accepted 1 Apr 2011; published 8 Apr 2011

18. B. Hou, Z. H. Hang, W. Wen, C. T. Chan, and P. Sheng, "Microwave transmission through metallic hole arrays: Surface electric field measurements," Appl. Phys. Lett. **89**(13), 131917 (2006).
19. T. J. Kim, T. Thio, T. W. Ebbesen, D. E. Grupp, and H. J. Lezec, "Control of optical transmission through metals perforated with subwavelength hole arrays," Opt. Lett. **24**(4), 256–258 (1999).
20. A. A. Yanik, X. Wang, S. Erramilli, M. K. Hong, and H. Altug, "Extraordinary midinfrared transmission of rectangular coaxial nanoaperture arrays," Appl. Phys. Lett. **93**(8), 081104 (2008).
21. T. Thio, H. F. Ghaemi, H. J. Lezec, P. A. Wolff, and T. W. Ebbesen, "Surface-plasmon-enhanced transmission through hole arrays in Cr films," J. Opt. Soc. Am. B **16**(10), 1743 (1999).
22. A. K. Azad, Y. Zhao, and W. Zhang, "Transmission properties of terahertz pulses through an ultrathin subwavelength silicon hole array," Appl. Phys. Lett. **86**(14), 141102 (2005).
23. A. Degiron, H. J. Lezec, W. L. Barnes, and T. W. Ebbesen, "Effects of hole depth on enhanced light transmission through subwavelength hole arrays," Appl. Phys. Lett. **81**(23), 4327 (2002).
24. T. W. Ebbesen, H. J. Lezec, H. Ghaemi, T. Thio, and P. A. Wolf, "Extraordinary optical transmission through sub-wavelength hole arrays," Nature **391**(6668), 667–669 (1998).
25. A. V. Itagi, D. D. Stancil, J. A. Bain, and T. E. Schlesinger, "Ridge waveguide as a near-field optical source," Appl. Phys. Lett. **83**(22), 4474–4476 (2003).
26. E. X. Jin, and X. Xu, "Finite-difference time-domain studies on optical transmission through planar nano-apertures in a metal film," Jpn. J. Appl. Phys. **43**(1), 407–417 (2004).
27. E. X. Jin, and X. Xu, "Enhanced optical near field from a bowtie aperture," Appl. Phys. Lett. **88**(15), 153110 (2006).
28. The numerical simulations are carried out using a finite-difference-time-domain package, Lumerical FDTD Solutions.
29. E. D. Palik, "Handbook of Optical Constants of Solids." (Academic, Orlando, FL, 1985)
30. M. Huang, A. A. Yanik, T. Y. Chang, and H. Altug, "Sub-wavelength nanofluidics in photonic crystal sensors," Opt. Express **17**(26), 24224–24233 (2009).
31. A. A. Yanik, M. Huang, A. Artar, T. Y. Chang, and H. Altug, "Integrated nanoplasmonic-nanofluidic biosensors with targeted delivery of analytes," Appl. Phys. Lett. **96**(2), 021101 (2010).
32. S. Aksu, A. A. Yanik, R. Adato, A. Altar, M. Huang, and H. Altug, "High-throughput nanofabrication of infrared plasmonic nanoantenna arrays for vibrational nanospectroscopy," Nano Lett. **10**, 2511–2518 (2010).

## 1. Introduction

Metamaterials have gained tremendous interest over the past few years due to their unusual electromagnetic properties, which can be useful for negative refractive index materials, perfect lensing, bio-sensing, and invisibility cloaking [1–4]. The electromagnetic properties of metamaterials are derived mainly from the resonating elements rather than atoms or molecules as in conventional materials [5]. Engineering metamaterials with multiple resonances that can be tuned from mid- to near-IR wavelengths could have in depth consequences for chip based optical devices, active filters, optical modulators, and bio-sensors [1–5]. The multi-resonant character of a metamaterial structure makes it particularly suitable for light control at several frequency ranges simultaneously [6–8]. A microwave dual-band negative-index metamaterial was fabricated [9] and experimentally confirmed as a multi-frequency resonator [10]. Recently, near-IR metamaterials with dual-band negative-index characteristics were also reported [11,12]. Obtaining such unique electromagnetic responses require investigation of novel metamaterial designs. As a result, many researchers have focused on subwavelength apertures, resulting in unusual high transmissions, in the optical [13,14], infrared [15], terahertz (THz) [16,17], and microwave [18] frequency ranges. The optical characteristics of the apertures are highly dependent on the refractive index of the adjacent medium [19], the shape and orientation of the apertures [20–22], metal film thickness [23], and lattice geometry [24–27].

In this study, we propose a compact metamaterial composed of integrated U- and T-shaped nano-apertures supporting multi-spectral resonances. We investigate the spectral response of this novel metamaterial antenna both numerically and experimentally. In order to understand the physical origin of the multi-resonant behavior, we analyze the structure by finite difference time domain (FDTD) method and obtain the field distributions of resonant modes. Strong near field enhancements are observed around the apertures. For further confirmation, we experimentally investigate the spectral responses of the individual U- and T-shaped nano-aperture antennas and compare the experimental results with the numerical analysis. We also determine the parameters that can enable fine control of the resonance frequencies. Due to the multi-spectral response and enhanced near field distributions, the proposed antennas can be useful for wide range of applications. Large field enhancements are

#142785 - $15.00 USD Received 16 Feb 2011; revised 29 Mar 2011; accepted 1 Apr 2011; published 8 Apr 2011

highly important for non-linear optics and sub-wavelength lithography. Similarly, multiple resonant bands can be important for wavelength-tunable filters as well as for advanced optical modulators and ultrafast switches operating at multiple wavelengths.

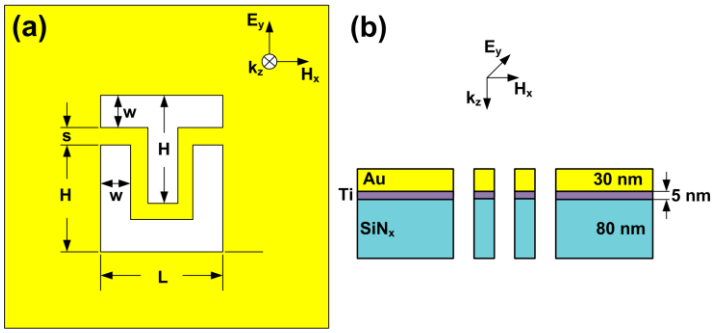


Fig. 1. The schematic view of the proposed UT-shaped metamaterial antenna design (a) Top view of the UT-shaped metamaterials including the geometrical parameters: L, the length, H, the height, w, the gap width, and s, the distance between the individual U- and T-shaped apertures. The y-polarized illumination source is indicated in the figure as well. (b) Side view of the proposed antenna geometry: 30 nm thick Au, 5 nm thick Ti, and 80 nm thick $SiN_x$ layers.

## 2. Numerical analysis and fabrication process of the UT structures

Figure 1 shows the schematic view of the proposed UT-shaped metamaterial antenna design. In this figure, L indicates the length of the structure, H indicates the height, w indicates the gap width, and s shows the distance between the individual U- and T-shaped apertures. We investigate the spectral response of the proposed antenna both numerically and experimentally. For the numerical analysis, the UT-shaped nano-aperture antennas are modeled by FDTD method [28]. During the simulations, the dielectric constants of Ti and Au are taken from ref [29]. In the unit cell, consist of the two individual elements, periodic boundary conditions is used along x and y axes and perfectly matched layers are used along z, the direction of the illumination source.

The scanning electron microscope (SEM) image and the optical responses of the fabricated nanostructures are shown in Fig. 2. Calculated and measured reflection spectra, given in Fig. 2(a) and 2(b), clearly show that the proposed nano-aperture antenna have multiple resonances ($\lambda_1$, $\lambda_2$, and $\lambda_3$) at the mid-IR wavelengths. These resonant dips can be well controlled by changing the physical properties of the apertures. For the experimental demonstration of the calculated multi-resonant characteristic, the proposed UT-shaped nano-aperture antennas are fabricated on a free standing 80 nm thick silicon nitride ($SiN_x$) membrane. Fabricated structures are characterized optically by a Fourier transform infrared (FTIR) microscope. Our experimental set-up consists of an IR microscope coupled to a Bruker$^{TM}$ FTIR spectrometer with a KBr splitter. Normally incident electromagnetic radiation, shown in Fig. 1, is used to efficiently excite the surface plasmon modes on the resonators. For $E_y$ polarized light (where E-field is parallel to the both arms of the U-shaped aperture) the structure provides three distinct resonances. While for $E_x$ polarization, there is only a dual-band resonant behavior (data not shown). Reflected infrared signal is collected by a Cassagrian reflection optics (NA = 0.4) and coupled into a liquid $N_2$-cooled mercury cadmium telluride detector. Reflection data are normalized using an optically thin gold standard.

#142785 - $15.00 USD Received 16 Feb 2011; revised 29 Mar 2011; accepted 1 Apr 2011; published 8 Apr 2011

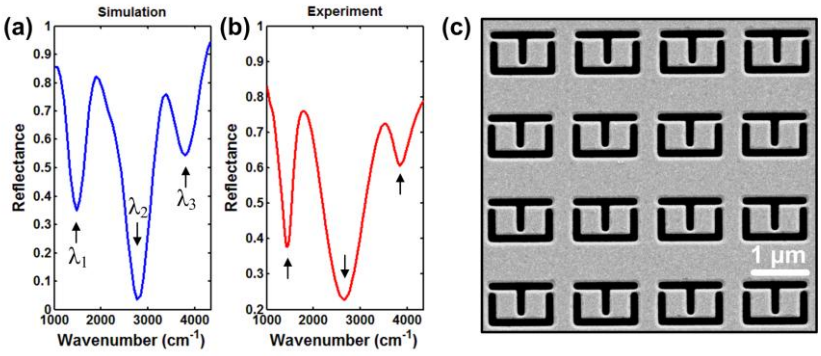


Fig. 2. Calculated and measured reflection spectra and SEM image of the proposed UT-shaped metamaterial antenna. (a) Numerical results obtained by FDTD method. (b) Experimental results for the UT-shaped nano-aperture antenna. Three distinct resonance modes are clearly observed both in simulation and experiment (indicated by arrows). The corresponding parameters are s = 180 nm, w = 120 nm, H = 720 nm, and L = 1200 nm. (c) SEM image of the fabricated structures.

The fabrication process is summarized in Fig. 3. In order to achieve high quality nano-structures, we use electron beam lithography (EBL). First, we fabricate the suspended $SiN_x$ membranes using photo lithography, reactive ion etching (RIE), and potassium hydroxide (KOH) etching, respectively. Then, nano-apertures are patterned on the membranes supported by UT-shaped nano-apertures using EBL with positive tone resist polymethylmethacrylate (PMMA). Later, these nano-apertures are transferred to $SiN_x$ layer by dry etching method. The rest of PMMA on the $SiN_x$ surface is removed by plasma cleaning, which results in free-standing nanostructures. The final step of our fabrication process involves direct deposition of the metallic layers of 5 nm-thick Ti and 30 nm-thick Au layers to obtain the plasmonic structures on the patterned membranes [30–32]. SEM images clearly show that the surface of the fabricated structures is smooth, apertures are well defined, and unit cells are uniform over large areas.

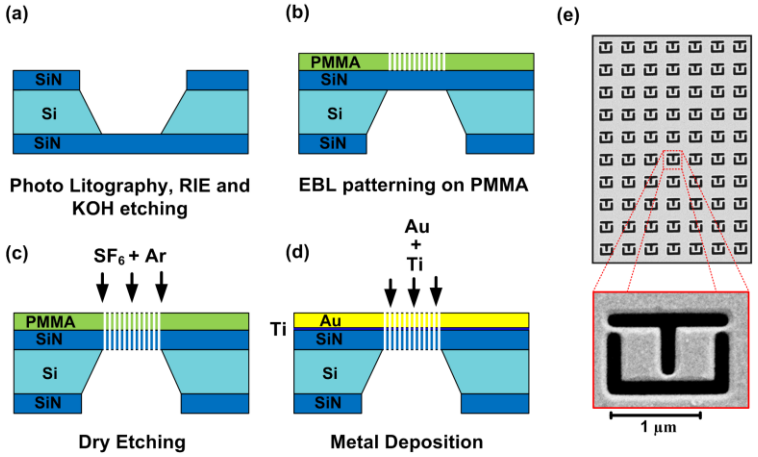


Fig. 3. Fabrication scheme and the SEM images of the UT-shaped nano-aperture antennas. To define a suspended $SiN_x$ membrane, (a) Photo lithography and RIE (dry) and KOH (wet) etchings are applied. (b) PMMA is spinned on the free-standing membrane, and then nanostructures are patterned on it by using EBL. (c) Apertures are formed after dry etching and $O_2$ plasma cleaning. (d) Directional metal deposition is used to obtain plasmonic structures with gold deposition of 30 nm-thick Au film after 5 nm-thick prior adhesion Ti layer. (e) SEM images of the UT-shaped nano-aperture array with a zoomed single unit cell.

#142785 - $15.00 USD Received 16 Feb 2011; revised 29 Mar 2011; accepted 1 Apr 2011; published 8 Apr 2011

## 3. Field distributions

In order to understand the physical origin of the multi-spectral response supported by UT-shaped nano-apertures, we perform numerical simulations using FDTD method. We show the field distributions corresponding to the resonance dips ($\lambda_1$, $\lambda_2$, and $\lambda_3$) indicated with arrows in Fig. 2. The z-component of the magnetic field intensities inside the metal layer, $|H_z|^2$, at the reflectance dips are shown in Fig. 4(a)-(c). These figures show that the first and the third modes are mainly located at the U-shaped aperture and second one is located at the T-shaped aperture. The lower order mode of the U-shaped structure has two strong lobes, which are located at the arm ends of the apertures. Similarly, the second mode, originated from the T-shaped nano-aperture antenna, has two strong lobes located at the ends of the upper arm of the T. On the other hand, the third mode which is the higher mode of the U-shaped aperture has four lobes, two of them are located at the arm ends and the rest is located at the corners of the aperture. Hence, the first and second modes of the compact structure are the fundamental modes of the individual nano-aperture antennas.

To determine the near field enhancement, we also show the total electric field intensities, $|E|^2$, of the three modes of the UT-shaped nano-aperture antennas in Fig. 4(d)-(f). The near field enhancements are larger than 1200 times for the first and second modes as shown in Fig. 4(d) and 4(e), which are highly desirable for Raman, fluorescence, and infrared spectroscopy. Furthermore, these field enhancements are mainly located within the apertures. This is highly desirable for biosensing applications as it increases the overlap of the analytes with the electromagnetic field inside the aperture.

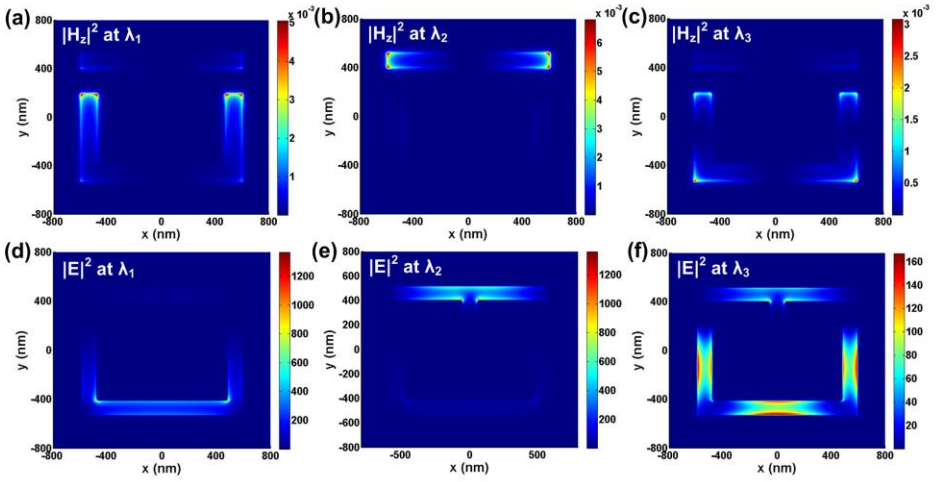


Fig. 4. Field distributions ($|H_z|^2$ and $|E|^2$) of the UT-shaped nano-aperture antennas inside the metallic layer (z = 15 nm) at the resonant modes of the structure with the corresponding parameters; s = 210 nm, L = 1200 nm, w = 120 nm and H = 720 nm.

## 4. Parameter dependence of the UT-shaped structures

As shown in Fig. 4, the fields in each resonance dip primarily concentrates at the individual elements of the compact UT structure. Hence, we obtain the spectral response of the individual elements both experimentally and numerically. Figure 5(a) and 5(b) show that the spectra of the U-shaped nano-aperture antenna have two separate resonances while the T-shaped nano-aperture supports only one resonant mode. The overall qualitative agreement between experiment and simulated results is quite good. Minor differences are likely due to fabrication tolerances in the experiment. To control the spectral response of the UT-shaped metamaterial antennas, we determine the dependence of the spectra on geometrical parameters including L, H, s, and w. In the compact antenna geometry, T-shaped nano-aperture antenna is vertically stacked into the U-structure. For this geometry, the control

#142785 - $15.00 USD Received 16 Feb 2011; revised 29 Mar 2011; accepted 1 Apr 2011; published 8 Apr 2011

parameter of the packing density is "s", which is the relative distance between the two individual elements (as illustrated in Fig. 1). The electromagnetic interaction between the individual resonators can be controlled by s which alters primarily the amplitude of the resonant dips. The strongest interaction is expected at the end of the vertically stacked arms of the resonators. The calculated reflection spectra are presented in Fig. 6 for different s values, while the other parameters are kept constant (L = 1200 nm, H = 720 nm, and w = 120 nm). As s decreases, the strength of the first and third order modes decreases significantly while the second mode shows negligible change. At s = 30 nm, due to the strong coupling between the individual elements, the compact structure loses its multi-resonant behavior. Increasing s allows the excitation of the two structures independently so that the lower and higher modes of the individual structures are clearly observed. According to the simulations, separation (s) within the range of 150 - 200 nm is sufficient enough to make a compact antenna that can support three distinct resonances.

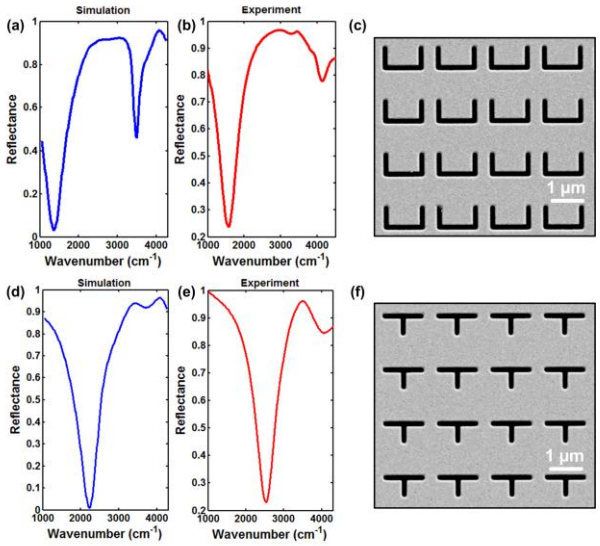


Fig. 5. Calculated and measured spectra and SEM images of the individual U- and T-shaped nano-aperture antennas. (a) Calculated, (b) measured spectra, and (c) SEM image of the U-shaped nano-aperture antennas (w = 190 nm, H = 800 nm, and L = 1650 nm). (d) Calculated, (e) measured spectra, and (f) SEM image of the T-shaped nano-aperture antennas (w = 190 nm, H = 800 nm, and L = 1620 nm).

We fabricated different UT-shaped nano-aperture antennas for the experimental investigation of the parameter dependence. The results of these experiments are illustrated in Fig. 7(a), 7(b), and 7(c), for w, H, and L, respectively. Increasing w slightly changes the resonance wavelengths while increasing H and L result in a strong red-shift in the reflection spectrum. Figure 7(d) shows that there is a linear relation between the resonance wavelength and the aperture length. According to the H dependence shown in Fig. 7(b), second order mode shows much weaker variations than the first and third modes. This can be inferred by analyzing the field patterns presented in Fig. 4. The field patterns for the second order mode are dominantly located at the corners of the upper arm of the T-shaped nano-aperture antenna. Therefore, changing height (H) which increases the tail of the T-aperture does not strongly effect the overall spectral position of the second mode. This is not the case for the first and third order modes as they are localized in the U-shaped apertures. As a result, calculated and measured reflection spectrums show that proposed metamaterial antenna has strong dips at the location of the resonant modes and the strongest one has been observed for the second mode. Although our proposed structure operate in mid-IR frequency range, by scaling the geometry

#142785 - $15.00 USD Received 16 Feb 2011; revised 29 Mar 2011; accepted 1 Apr 2011; published 8 Apr 2011

of the compact structure, the resonance locations can be tuned over a wide range, from mid-IR to visible wavelengths.

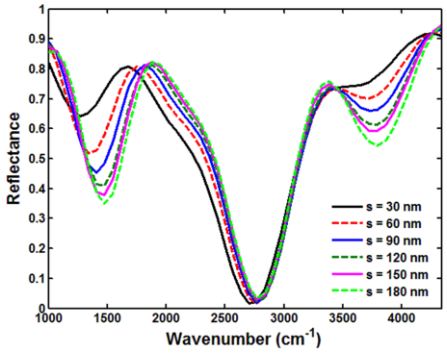


Fig. 6. Calculated reflection spectrum of the UT-shaped nano-aperture antennas for different s values (L = 1200 nm, H = 720 nm, and w = 120 nm).

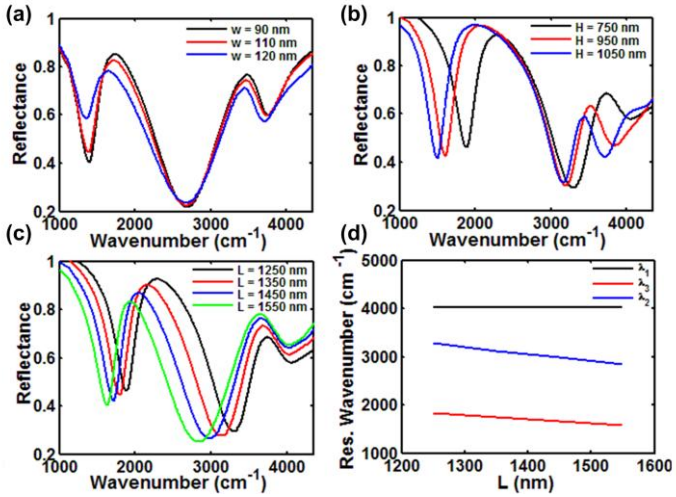


Fig. 7. Measured reflection spectra of the UT-shaped nanoaperture antennas for different cases (a) s, L and H are fixed while w is varied (L = 1250 nm, s = 140 nm, and H = 750 nm) (b) s, w and L are fixed while H is varied (L = 1250 nm, s = 140 nm, and w = 230 nm) and (c) s, w, and H are fixed while L is varied (H = 750 nm, s = 140 nm, and w = 230 nm) (d) The three resonance dips ($cm^{-1}$), $\lambda_1$, $\lambda_2$, $\lambda_3$ as a function of length (nm) (H = 750 nm, s = 140 nm, and w = 230 nm).

## 5. Conclusion

In conclusion, we introduce a novel multi-resonant metamaterial design based on coupled U- and T-shaped nano-apertures. The resonant modes can be easily tuned to the desired frequencies by simply changing the structural parameters of the apertures. Such metamaterials with tunable resonances from mid-IR to visible wavelengths could have far-reaching consequences for chip based frequency selective optical devices including active filters, optical modulators, and bio-sensors. Finally, our design shows high near-field resolution, which can be useful for sub-wavelength lithography, near field imaging and surface enhanced spectroscopy.

#142785 - $15.00 USD Received 16 Feb 2011; revised 29 Mar 2011; accepted 1 Apr 2011; published 8 Apr 2011

**Acknowledgments**

We gratefully acknowledge support from NSF CAREER Award (ECCS-0954790), ONR Young Investigator Award, Massachusetts Life Science Center New Investigator Award, NSF Engineering Research Center on Smart Lighting (EEC-0812056) (HA) and The Council of Higher Education of Turkey (YOK) (MT).

#142785 - $15.00 USD Received 16 Feb 2011; revised 29 Mar 2011; accepted 1 Apr 2011; published 8 Apr 2011